Available online at www.sciencedirect.com
SCIENCE DIRECT
Polymer 46 (2005) 705–712
polymer
www.elsevier.com/locate/polymer

Effect of shear history on the morphology and coarsening behaviour of polycarbonate/poly(styrene-*co*-acrylonitrile) blend

Gehan M. Hanafy[a], Samy A. Madbouly[a,c,*], Toshiaki Ougizawa[a], Takashi Inoue[b]

[a]*Department of Organic and Polymeric Materials, Tokyo Institute of Technology, 2-12-1 O-okayama, Megruo-ku Tokyo 152-5882, Japan*
[b]*Department of Material Science and Engineering, Yamagata University, Yonezawa 992-8510, Japan*
[c]*Chemistry Department, Faculty of Science, Cairo University, Orman-Giza, 12613, Egypt*

Received 10 August 2004; received in revised form 27 November 2004; accepted 2 December 2004
Available online 19 December 2004

Abstract

The morphology and coarsening behaviour of polycarbonate (PC) blend with styrene-*co*-acrylonitrile (SAN) random copolymer of 25 wt% AN have been investigated as a function of shear history using transmission electron microscope (TEM) and time resolved light scattering techniques. Simple shear apparatus of two parallel plates geometry was used to generate different shear rate values depending on the different distances from the centre of the sample disk. The morphology of PC/SAN-25 = 70/30 blend showed that the dispersed phase of SAN was elongated and broken-up in the direction of flow with weaker contrast at high shear rate values. The shear rate was found to suppress the concentration fluctuations and enhance the miscibility of SAN (dispersed phase) in the PC matrix to a great extent. The average of the dispersed particle diameter was evaluated as a function of different shear memories at 240 °C for different time intervals based on the Debye–Bueche theory. The obtained data were found to be shear memory dependent i.e. the average particle diameter decreases with increasing shear memory. This result indicated that the coarsening process is greatly suppressed by shear memory and the shear could produce a permanent morphological change (irreversible change) over the time scale of the measurement. This behaviour was attributed to the very high melt viscosities of the blend components, which in turn led to a very long relaxation time and consequently a high difficulty to erase the effect of shear at the experimental temperature. Furthermore, the coarsening process for all the measured samples followed the general power law, $\bar{R}^3(t) = \bar{R}^3(0) + t$, regardless of the shear memory of the blend. This behaviour implied that the shear could only retard the rate of domain growth without any effect on the coarsening mechanism.

Keywords: Shear history; Coarsening behaviour; Particle size

1. Introduction

Most polymer mixtures are immiscible and separated into two-phase morphology. Immiscible blends with coarse, irregular, and unstable domain sizes with sharp and weak interface produce poor properties and practical incompatibility. However, on the other hand, when a two-phase blend has naturally good properties and practical compatibility, the reason is usually to be sought in partial miscibility. The compatibility of polymer blends can be improved by controlling the processing conditions i.e. temperature, shear flow, and mixing time during the mechanical mixing of the molten polymers. Where the final phase morphology is greatly influenced by those major factors and the final quenching materials may freeze-in a non-equilibrium state. Therefore, it is not surprising that different research groups may report different degrees of success or failure when using such a physical process as only a force for enhancing the miscibility. Controlling the processing condition is of industrial relevance in the processing and production of polymer blends, where temperature gradients and high deformation rates are encountered as in melt extrusion or injection moulding. Thus, the behaviour of blends in flow field is of a fundamental interest and also technologically important, since deformation and related stresses are

* Corresponding author. Address: Department of Organic and Polymeric Materials, Tokyo Institute of Technology, 2-12-1 O-okayama, Megruo-ku Tokyo 152-5882, Japan. Tel.: +81 357 342 439; fax: +81 357 342 423.
E-mail address: samy@o.cc.titech.ac.jp (S.A. Madbouly).

0032-3861/$ - see front matter © 2004 Elsevier Ltd. All rights reserved.
doi:10.1016/j.polymer.2004.12.005

unavoidable in many processing steps. The flow field was found to exert a marked influence on the morphologies of blends and it is apparent that this effect must be taken into account, in particular in understanding the state of polymer blends during processing.

In recent years significant emphasis has been placed on the processing role that can be played in controlling the possibly modifying, in a predictable manner, the microstructure of fabricated components made of polymer blends. Flow processing, in particular, is seen as a flexible means of generating verity of microstructures from the same raw materials in reproducible, inexpensive and continuous ways. A huge number of literature studies have inferred the influence of shear flow on the microstructure of two-phase blends and composites [1–5]. The majority of these studies have been investigated for not well controlled flow conditions; such as those encountered in batch mixers, extruders and injection moulding, where both shear flow and extension flow are accompanied during the processing. Therefore, only qualitative analysis for the relationship between morphology and flow parameters (shear rate) has been proposed. Based on this fact, it is apparent that, morphological study of polymer blends under well-controlled flow conditions is difficult and relatively scarce in the literature.

The coarsening is a process observed to control the late stages of morphological development of wide variety of two-phase systems. The driving force of coarsening process is the tendency to decrease the total interfacial area, and concomitantly, the system energy. An increase in the average particle size and a decrease in the number of particles are accompanying the process. The consequence of events is typically phase segregation of the two-phase system by spinodal decomposition (SD) or nucleation and growth followed by coarsening. The coarsening process can occur under both quiescent and flow condition. The dispersed particle diameter increases with concentration, interfacial tension, and decreases with shear stress. The coarsening process of multiphase polymer blends has been observed and commented quantitatively [6–11].

Blend of polycarbonate, PC, and acrylonitrile-butadiene-styrene terpolymer (ABS) has been commercially available for many years [12–16]. This blend showed excellent properties without any compatibiliser; such as, a suitable block or graft copolymer for interfacial modification, which is necessary for most of commercial immiscible blends. The useful properties of PC and ABS raised a considerable interest on the nature of the interaction between PC and styrene-*co*-acrylonitrile (SAN), which represents the matrix of ABS. Since, it is believed that the favourable thermodynamic interaction between PC and SAN is the most responsible factor for the excellent properties of the blend without any modification.

We previously [17] systematically investigated the miscibility and morphology of PC and SAN copolymer with different AN contents ranging from 11–74 wt%. PC and SAN could form partial miscible blend depending on the AN content, blend composition and shear rate. The finest phase dispersion of PC/SAN = 70/30 blend under same processing condition was observed at AN wt% 25. The viscosity ratio of PC/SAN = 70/30 blends of different AN contents (η_{SAN}/η_{PC}) was found to play a minor role for controlling the blend morphology. The optimum interaction between PC and SAN at AN wt% 25 was the only factor responsible for the observed finest morphology.

In the current work, the coarsening behaviour of PC/SAN-25 = 70/30 blends will be investigated at 240 °C using a time resolved light scattering technique and transmission electron microscope. The miscibility and morphology of the blends will be studied under different simple shear values. In addition, the effect of different shear memories on the coarsening process will be also considered in this work. It is expected that the shear memory might be preserved even after shear cessation and could be affected by the rate of domain growth of the dispersed SAN phase in the PC matrix.

2. Experimental section

2.1. Materials and samples preparation

The PC sample was obtained from Mitsubishi Gas Chem. Cop., Japan with $M_w = 37{,}000$ g/mol and $M_w/M_n = 1.4$. The SAN sample was obtained from Mitsubishi Monsato Cop., Japan with 25 wt% acrylonitrile. The M_w and M_w/M_n of SAN sample were 128,000 g/mol and 2.1, respectively.

The samples were dried under vacuum for 3 days at 80 °C before using. About 0.5 g of the total blend weight was then taken and melt mixed at 240 °C for 5 min using a min–max moulder machine (Custom Scientific Instruments, Inc., Cedar Knolls, NJ, Model CS-183 MMX) [18]. The rotor speed was fixed at 100 rpm for preparing all the samples. Under this mixing condition the calculated shear rate value is approximately 10 s^{-1}. After each mixing time the sample was picked up quickly and quenched in a water bath. This value of shear rate was found to be not enough to enhance the miscibility of the blend as it was previously reported under this condition [17].

About 0.5 g from the quenched blend of the mini-max moulder was taken and pressed at 200 °C for a short time (about 2 min) to prepare a disk specimen of 0.4 mm thickness and 40 mm diameter for high shear rate measurements up to 90 s^{-1}.

2.2. Shear apparatus

The details of the shear apparatus have been described elsewhere [19]. The sample is located between two parallel glass plates, the top one is fixed and the bottom one is rotated by different rotation speeds controlled by the motor and gear mechanism. The simple shear flow is generated by

applying a constant rotation speed of 0.6 rad/s for 5 min to the sample, which was preheated at 240 °C. For the parallel plate measurements, the shear rate is a linear function of the radius

$$\dot{\gamma} = \Omega r/h \quad (1)$$

where h is the sample thickness, r is the radius, and Ω is the rotation speed (rad/s). The shear rate is a maximum at the outer edge of the disk (r=R) and decreases to zero at the center of the disk (r=0). Once the measurement was finished, the two plates with the sample could be released very quickly to allow rapid quenching in a water bath for the transmission electron microscope (TEM), thermal analysis (DSC) and light scattering measurements.

2.3. Morphology

For the TEM analysis, small specimens of different radial positions from the quenched sample disk (different shear rate values) were then taken and microtomed to an ultrathin of 70 nm thickness using a Reichert–Jung ultracryomicrotome with a diamond knife, and then they were stained by RuO_4 vapour. The structure in the section was observed under TEM, JEM 100CX (100 kV).

2.4. Thermal analysis

The thermal analysis was investigated calorimetrically for the quenched samples of various shear memories using a DSC (Seiko instruments EX ST R 6000). The heating rate was 10 °C/min for all measurements. The T_g was defined as the temperature of the half of step height in specific heat curve.

2.5. Light scattering measurements

For the light scattering measurements, the specimens of different shear memories (different radial positions from the centre of the sample disk) were placed between two cover glasses and melt-pressed to a thin film (about 40 μm thick) on a hot chamber kept at a constant temperature (240 °C) and was annealed. After that, the melt-pressed specimens were subjected to the time resolved light scattering measurement in a direction normal to the flow. Radiation from a He–Ne gas laser of 632.8 nm wavelength was applied vertically to the film specimen. The goniometer trace of the scattered light from the sample specimen was obtained under a V_v (parallel polarised) optical alignment. Thus, the change in the light scattering profile was recorded as appropriate intervals during the isothermal annealing. A detail of our light scattering device has been described elsewhere [20].

2.6. Viscoelastic measurements

Disk specimens of 1 mm thickness and 25 mm diameter were prepared from the dried pure polymer components at 200 °C for the viscoelastic measurements. The steady shear viscosity (η) was measured by a rheometrics dynamic mechanical spectrometer (model RDA 2) using 25 mm parallel plates-diameter. The measurements were carried out at a shear rate range of 0.05–100 s^{-1} at 240 °C.

3. Results and discussion

3.1. Morphology under shear flow

The morphology of two-phase structure under a controlling shear condition is attracted a considerable attention in recent years. Here the effect of simple shear flow on the morphology and miscibility of PC/SAN-25=70/30 blend will be investigated under simple shear flow. The simple shear flow measurement was carried out at 240 °C under constant rotation speed of 0.6 rad/s for 5 min and after that the sample taken out from the hot shearing chamber quickly to allow a rapid quenching in a water bath. Four pieces were then taken from different radial positions of the disk, and their morphologies were then achieved by TEM on the ultramicrotomic slices cut parallel to the flow direction.

Typical morphological observations of the samples under different values of shear rate are shown in Figs. 1a–d. The bright dispersed phase and dark matrix are corresponding to SAN (not stained) and PC (stained by RuO_4), respectively. It is clear that, a well-defined phase separation of the blend at a nearly zero shear rate (centre of the disk) can be obtained. For the samples under shear, the particles are oriented to the flow direction and the size strongly dependent on shear rate. These results can be classified into two regimes I to II according to the shear rate values. In

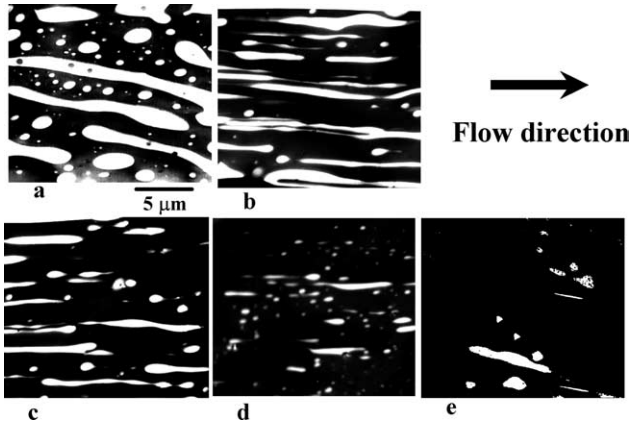

Fig. 1. TEM pictures of PC/SAN-25=70/30 samples that were sheared at 240 °C by different shear rates for 5 min and then quenched in water bath. Five pieces were then taken from different radial positions and consequently different shear rates (a)$\dot{\gamma} \approx 0\ s^{-1}$; (b) 7.5 s^{-1}; (c) 15 s^{-1}; (d) 30 s^{-1} and (e) 90 s^{-1}.

regime I, at a nearly zero shear rate (centre of the disk) the blend separated into two phases of SAN dispersed and PC matrix. Regime II at 0.5, 1 and 2 cm from the centre of the disk and shear rates of 7.5, 15 and 30 s^{-1}. In this regime the transmission electron micrograph indicates break-up of the bigger domains into smaller ones whose characteristic shows high degree of orientation in the direction of flow. Based on the morphology obtained in Fig. 1, one can conclude that, macroscopic phase separation could not occur under steady shear flow. With increasing the shear rate the macroscopic phase boundary is broken into pieces generating smaller domains which can be elongated in the flow direction, resulting in loosing the contrast and intensity of the elongated phases i.e. decreasing the concentration fluctuations, and consequently the mixing of the unlike segments is enhanced.

The morphology under high shear rate values (up to 90 s^{-1}) does not change so much as seen in Fig. 1e. This may be attributed to the fact that, the sample under higher shear rate seems to be under quasi-equilibrium condition and the morphology might be controlled by two competitive factors. One tries to break-up the domains into smaller ones i.e. shear-induced break-up of the dispersed domains. The other tends to increase the rate of domain growth i.e. shear-induced coalescence. The competition between the two factors leads to same morphology at shear rate higher than 30 s^{-1}. Therefore, the morphology of Fig. 1e can be considered as the quasi-equilibrium morphology that can be controlled by the competition between shear-induced break-up and shear-induced coalescence.

Based on the above, it is apparent that the shear-induced break-up is the only phenomenon carried out at small shear rates. The particle size decreased strongly with increasing shear rate up to 30 s^{-1}. This sharp decrease in the particle size in this range should not take place if there is a possibility for shear-induced coalescence at small shear rate values. However, it might also be correct to say that shear-induced break-up is predominant at small shear rate values and the competition between shear-induced break-up and coalescence becomes significant at high shear rate values.

3.2. Viscoelastic properties

Fig. 2 demonstrated the steady shear viscosity for the two polymer components used in this work at 240 °C (similar to the shear temperature) in a double logarithmic scale. The viscosity ratio is the most important rhelogical parameter, which can control the morphology of immiscible polymer blends. The effect of viscosity ratio on the final phase morphology of two-phase systems has been extensively investigated in the literature [21–25] and it is well established that the minimum domain size of the dispersed phase is obtained at a viscosity ratio of approximately unity.

Taylor developed a theory for break-up of a single Newtonian droplet of diameter D in a simple shear flow, the balance between viscous and interfacial forces is used to control the droplet size and break-up [26,27]. The resulting is a well-established dimensionless parameter and is called Capillary number, Ca:

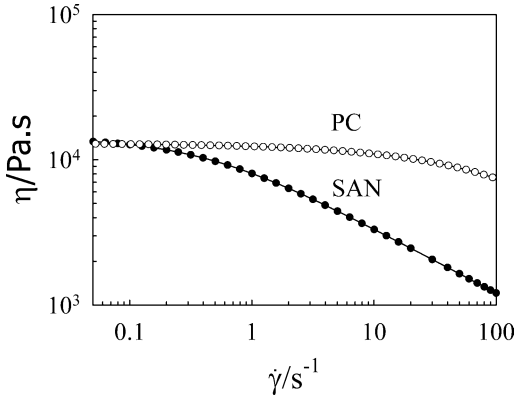

Fig. 2. Steady shear viscosities as a function of frequency for PC and SAN-25 at 240 °C.

$$\mathrm{Ca} = \frac{\eta_m \dot{\gamma} D}{2\sigma} \tag{2}$$

where $\dot{\gamma}$ is the shear rate, D is the diameter of the droplet and σ is the interfacial tension. Two different situations can be obtained from the above equation depending greatly on the value of Ca. The first one is deformed droplet, when the two stresses balanced each other, this occurred at small value of Ca. The second case for large value of Ca, the viscous forces dominate, causing the irreversible deformation of the drop, which will eventually break-up into smaller domains. The value of Ca was estimated as function of viscosity ratio in both simple shear and extension flow by Grace [28]. It was found that Ca is a strong function of viscosity ratio $\eta_r = \eta_d/\eta_m$ (η_d is the viscosity of dispersed phase and η_m is the viscosity of the matrix) and reaches a minimum value at $\eta_r \approx 1$, indicating that the maximum rate of the dispersed phase to break-up is occurred when the dispersed and continuous phase have almost same viscosity. His result also confirmed that droplet break-up is impossible in simple shear flow above $\eta_r = 4$.

Droplet collision, which leads to coalescence, might be occurred also during shear flow that caused by Brownian motion and dynamics of concentration fluctuations. Most of literature data reported that the equilibrium droplet diameter should increase with concentration, interfacial tension coefficient, and decrease with shear stress. Elmendorp et al. [29,30] predicted that coagulation results from collision of two droplets of diameter D takes place when they approach each other less than the critical distance. They also confirmed that the coagulation time increases with the matrix viscosity and with the diameter of the droplet but decrease with an increase in the interfacial coefficient. Therefore, the coalescence of two isolated drops is easier for smaller spheres with high interfacial energy.

The value of viscosity ratio for PC/SAN = 70/30 blend (η_{SAN}/η_{PC}) ranged from 1 at low shear rate to 0.17 at high

shear rate. The changing of shear rate leads to a significant change in the value of viscosity ratio. Therefore, the rate of droplet break-up at small shear rate value is very high and predominant but, it decreases at higher shear rate. Based on the above the droplet break-up and coalescence balanced each other at high shear rate. This is why no shear-induced one-phase morphology could be detected at a high shear rate as shown in Fig. 1e.

This rheological data can be considered as convincing evidence that the shear-induced coalescence is occurred at high shear rates. Since if only a phenomenon of shear-induced break-up takes place at high shear rates, this means the particle size should be decreased gradually with increasing the shear rate. At a certain shear rate value (critical shear rate) we will not be able to detect the morphology by any experimental method such as TEM or light scattering and consequently a formation of miscible blend with a single T_g. But this is not the case as seen in Fig. 1 i.e. two-phase morphologies at all values of shear rates are observed. Therefore, the competition between shear-induced break-up and coalescence is very significant and plays a major role to control the morphology of the blend at high shear rates. In previous studies we could obtain one phase blend (no morphology could be detected by TEM) at high shear rates for two different blends of PMMA/SAN and PMMA/PαMSAN because there was no any shear- induced coalescence occurred [31,32].

3.3. Thermal analysis

The DSC measurements for the five pieces of different shear memories (the same samples of Fig. 1) are shown in Fig. 3. One can see that all pieces exhibit two T_g's of the SAN-rich and PC-rich phases. The T_g of the SAN-rich phase is almost constant at all values of shear rate, indicating no more PC is dissolved in the SAN-rich phase. However, on the other hand, the T_g of the PC-rich phase is shifted to lower temperature with increasing the applied shear rate values. The reason of this shift is attributed to the fact that some amount of SAN dissolved in PC under shear. For the sample prepared by solvent cast method no shift could be detected. So this shift suggests that the miscibility of SAN in PC can be improved under shear flow in good agreement with the above morphology (Fig. 1).

From the DSC measurements one can estimate the amount of SAN dissolved in PC as a result of shear flow by applying Fox Equation [33]

$$\frac{1}{T_g} = \frac{w_{SAN}}{T_{g\ SAN}} + \frac{1 - w_{SAN}}{T_{g\ PC}} \tag{3}$$

after rearrangement one can obtain the following relation

$$w_{SAN} = \frac{T_{g\ SAN}(T_{g\ PC} - T_g)}{T_g(T_{g\ PC} - T_{g\ SAN})} \tag{4}$$

where $T_{g\ SAN}$ and $T_{g\ PC}$ are the glass temperatures of pure SAN and PC, respectively, and T_g is the glass temperature of PC-rich phase. Fig. 4 shows the shear rate dependence of percent weight of SAN dissolved in PC-phase. It is apparent that the dissolved-SAN percent increases strongly with shear memory in the moderated shear range and then levels off at high shear memories. This behaviour is in good agreement with the morphology of Fig. 1, since the improvement in the morphology of the blend reached a maximum at a shear memory of 30 s^{-1} and does not change at higher values.

3.4. Coarsening behaviour after shear cessation

The coarsening behaviours for three different pieces of different shear memories i.e. 0, 15 and 30 s^{-1} have been investigated using a time resolved light scattering technique in a direction normal to the flow. The light scattering data can be analysed on the basis of Debye–Bueche theory [34]. Series of morphological parameters, such as, correlation distance, ξ, specific interaction area, S_{sp}, and mean diameter of dispersed particle, $\bar{D}$, can be obtained from this theory. The scattering light intensity of two-phase system with irregular particle size is given by;

$$I(q)^{-1/2} = (8\pi\langle\eta^2\rangle\xi)^{-1/2}(1 + \xi^2 q^2) \tag{5}$$

where q is the magnitude of the scattering vector, given by

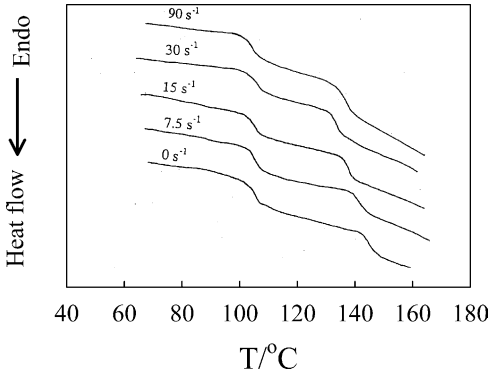

Fig. 3. DSC thermograms for PC/SAN-25 = 70/30 blends of different shear memories.

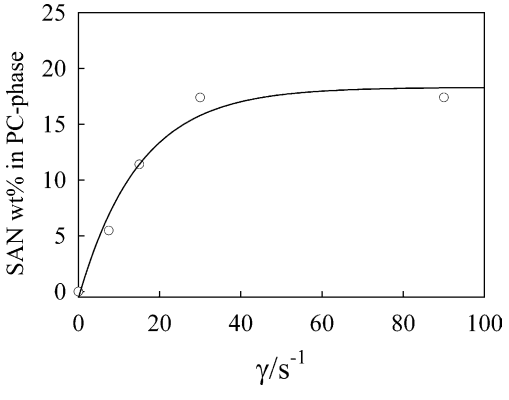

Fig. 4. Shear rate dependence of the amount of SAN wt% dissolved in PC-phase.

$q = (4\pi/\lambda')\sin(\theta/2)$, λ' being the wavelength of light in the specimen, $\langle\eta^2\rangle$ is the mean-square fluctuations of the relative index, and ξ is the correlation distance. The correlation distance, ξ, can be obtained from the slope and intercept of the linear relation between $I(q)^{-1/2}$ vs. q^2. Once the value of ξ is given; the other morphological parameters ($S_{sp}, \bar{D}$) can be deduced from the following relations;

$$S_{sp} = 4\phi(1-\phi)\xi^{-1} \quad (6)$$

and

$$\bar{D} = 6\phi S_{sp}^{-1} \quad (7)$$

where ϕ is the volume fraction of the dispersed phase.

It must be mentioned here that, the pure coalasence process can be demonstrated from the light scattering data only perpendicular to the flow direction. However, on the other hand, more than one phenomenon takes place in the direction parallel to the flow. The particle diameters parallel to the flow are very big due to the highly elongated domains. These highly elongated domains are broken-up during the first few minutes of the measurement into smaller particles with keeping the diameters of the particles perpendicular to the flow direction constant. After that the coarsening process proceeds with time. Therefore, the light sacttering data parallel to the flow direction is very complicated and difficult to analyse.

A typical experimental data for the coarsening time dependence of the average domain diameters of the blends under different shear memories normal to the direction of flow is shown in Fig. 5. The origin of the shear memory is shear rate dependence of concentration of SAN in PC and the concentration difference at the initial time when the coarsening starts. One can see that the coarsening process is strongly affected by shear memory. The coarsening process is significantly retarded with increasing the shear memory. This behaviour is reasonable and attributed to the fact that the shear rate could be suppressed by the concentration fluctuations and break-up the bigger domains into smaller ones and consequently retard the coarsening process of the blend. Based on the above result it appears that the shear

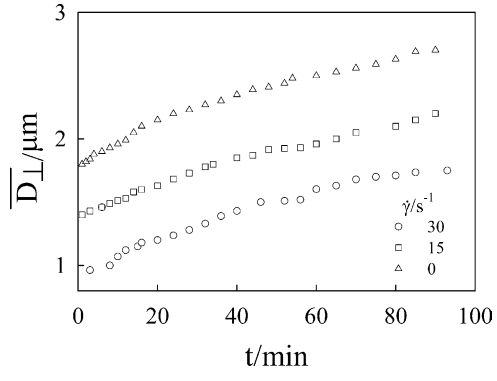

Fig. 5. Residence time dependence of the scattering particle diameters of PC/SAN-25=70/30 blends for different shear memories in a direction normal to the flow at 240 °C.

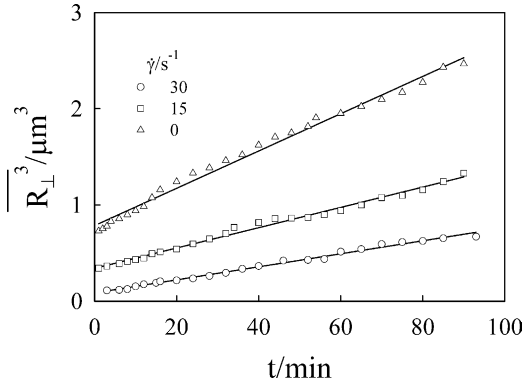

Fig. 6. Residence time dependence of the cub of the average particle radii of PC/SAN-25=70/30 blends for different shear memories in a direction normal to the flow at 240 °C.

memory of the blend is preserved even after shear cessation. This may be due to the very high melt viscosity of the blend at the experimental temperature, which leads to a very long relaxation time. The relaxation time here means that the time necessary for the concentration of SAN in PC to become the equilibrium value without shear rate. Therefore, the erasing of the shear effect seems to be partially over the time scale of the measurement.

The coarsening process proposed for droplet phase separation has been investigated by two different mechanisms [35,36]. The first one is the evaporation–condensation mechanism, which is known as Ostwald ripening [35]. The second is collision and coalescence, which is called Binder–Stauffer mechanism [36]. During Ostwald ripening (evaporation–condensation) mechanism, small droplets dissolve and large ones grow; centres of mass of particles are stationary, though 'evaporation' will cause the smallest to disappear. This type of coarsening originates from concentration gradients in the matrix, which are related to particle radius. On the other hand, coarsening process by collision and coalescence takes place when the dispersed particles move through the matrix and collide with one another to form fewer, larger droplets. This collision and coalescence between droplets is caused mainly by the free thermal diffusion of droplets without any interaction. Both

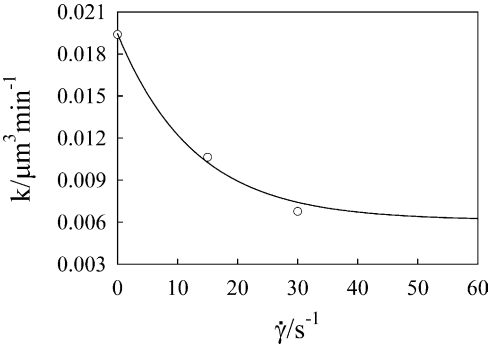

Fig. 7. Shear rate dependence of the coarsening rate obtained from the slopes of the curves of Fig. 6.

mechanisms give the same general power law:

$$\bar{R}^3(t) = \bar{R}^3(0) + kt \quad (8)$$

the cube of the average particle radius $\bar{R}^3$ increases linearly with time, $\bar{R}^3$ (0) is the initial value at $t=0$ The $t=0$ is arbitrary, provided liquid–liquid phase separation has been completed. K is the coarsening constant, which depends on mechanism, as well as temperatures, volume fraction of the dispersed phase, etc.

A typical experimental data for the coarsening process under different shear memories at 240 °C are plotted as $\bar{R}^3$ vs. t, normal to the direction of flow in Fig. 6. The results show linear relations, in accord with Eq. (8). Obviously, the coarsening process of the two phases is suppressed at higher shear rate i.e. the rate of domain growth decreases with increasing shear memory. One can calculate the coarsening constant at different shear memories from the slopes of the curves. It is apparent that the slope k decreases with shear memory as shown in Fig. 7 indicating that the rate of domain growth decreases at high shear memory. Thus, the effect of shear memory is seemed to be not altered by the mechanisms of the dispersed particle growth but simply to retard the rate of such growth. The shear memory dependence of the domain size normal to the direction of flow ($\bar{D}_\perp$) at different time intervals is shown in Fig. 8. Obviously the domain size decreases with shear memory; this result is consistent with the effect induced by shear rate on the morphology (see Fig. 1). The higher the shear rate the smaller the domain size.

According to these experimental facts one can conclude that, the shear memory strongly affects the coarsening process of PC/SAN blend. In addition, the shear could produce a permanent change to the two-phase morphology. However, a slow molecular diffusion rate, indicative of the high melt viscosity would also give an apparent non-revesiblity change over the time scale of the measurements.

Here we shall discuss the probability to erase the shear effect by allowing the sample to relax at high temperature for different time interval after the shear cessation. The sample is sheared at $T=240$ °C for 5 min, after that the shear is stopped and the sample allowed to relax at the same temperature for different time interval ranged from 5 to 20 min. After each relaxation time, the sample was taken out from the hot shear chamber quickly to allow a rapid quenching in a water bath. The morphology of the sample at 2 cm from the centre (30 s^{-1}) is investigated in each case, as shown in Fig. 9. Obviously with increasing the relaxation time, the orientation of the elongated particles of SAN decreases but cannot be completely vanishing even for 20 min after shear cessation. It was expected that the shear effect induced by the relatively low shear rates, would be completely erased by relaxation. But the experimental results indicate that the shear effect can be erased only partially. This may be again attributed to the high molecular weight and high viscosity of the blend at the experimental

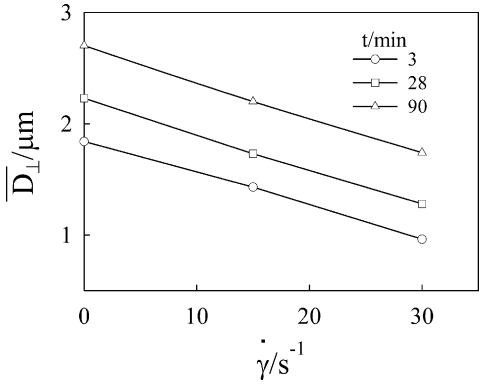

Fig. 8. Shear rate dependence of the average particle diameter at 240 °C for different annealing time.

temperature, which in turn led to a very slow relaxation. This morphology may be explained by two different processes, the first one is phase segregation i.e. molecular diffusion of SAN from PC-rich phase to SAN-rich phase, which starts immediately after shear cessation. The second one is a coarsening process, which leads to large domains with increasing annealing time.

According to the above discussion, one can say that, the complete erasing of the shear effect depends on the molecular weight and the viscosity of the blend at the experimental temperature and consequently on the relaxation times. The higher the viscosity, the longer the relaxation time, and the higher the difficulty to erase the shear effects completely.

Fig. 10 shows the effect of annealing time on the total SAN-rich area at 240 °C after shear cessation obtained from the image analysis of Fig. 9. Obviously the SAN-rich area increases abruptly within the first few minutes after shear cessation (up to 5 min) and then the rate of SAN-rich area increases slowly with time. This behaviour can be seen very

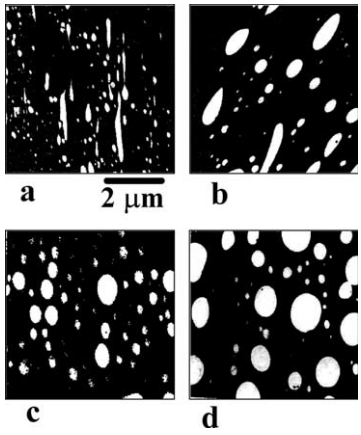

Fig. 9. TEM pictures of PC/SAN-25=70/30 samples that were sheared at 240 °C by 30 s^{-1} for 5 min and then the samples were allowed to relax at same temperature for different time intervals (a) 0 min; (b) 5 min; (c) 10 min and (d) 20 min.

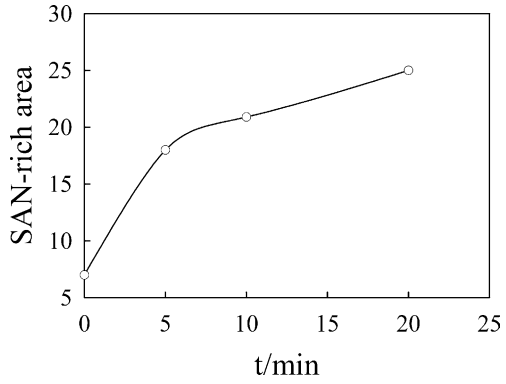

Fig. 10. Total SAN-rich areas as a function of annealing time at 240 °C after shear cessation of 30 s^{-1}.

clearly from the large change in the slope of Fig. 10 which confirmed the occurrence of two different processes after shear cessation. The first one is a rapid phase segregation process, which occurred immediately after shear cessation. This process is very fast, faster than the normal coarsening process, and has a large slope (see the initial slope of Fig. 10 in its first few minutes). The second process is a normal coarsening process, which is a characteristic for the blend in the late stage of phase separation. This process occurs after about 5 min from the shear cessation and has a small slope compared to the first process (phase segregation). The presence of these two processes may be attributed to the fact that the morphology of the blend after shear cessation is not completely two-phase structure but it is a partially miscible one as confirmed in Figs. 1 and 3. Therefore, the real coarsening process needs a certain time after which the blend may be changed to the late stage of phase separation (a completely two-phase structure). This time may be the time which needed for the phase segregation process.

4. Conclusion

The partial miscibility of PC/SAN-25 was enhanced to a great extent under moderate shear values up to 30 s^{-1}. However, on the other hand, no shear-induced one-phase structure was detected under high shear rate values. The shear memory could greatly suppress the coarsening behaviour of the blend. The obtained results seemed to be reasonable and consistent with the suppression of concentration fluctuations and broken-up the dispersed domains under shear flow. However, the shear could not change the coarsening mechanism, as seen in the linear relationship between $\bar{R}^3$ vs. t. The shear memory could not be erased after shear cessation but was preserved even at high temperature for long time as observed from the decreasing of the coarsening constant (slope of $\bar{R}^3$ vs. t). This might be attributed to the high melt viscosities and molecular weights of the blend components, which in turn led to slow molecular diffusion rate and non-reversible change of the shear effect over the time scale of the measurements. The morphological structures observed by TME after shear cessation confirmed the occurrence of two different processes. The first one is a rapid phase segregation process, which occurred immediately after shear cessation. The second process is a normal coarsening process, which is a characteristic for the blend in the late stage of phase separation.

Acknowledgements

Samy A. Madbouly is very grateful to the Japan Society for the Promotion of Science for supporting his stay in Japan.

References

[1] Sundararaj U, Macosko WC. Macromolecules 1995;28:2647.
[2] Favis BD, Chalifoux JP. Polym Eng Sci 1987;27:1591.
[3] Utracki LA, Shi ZH. Polym Eng Sci 1992;32:1824.
[4] Rivera-Gasetelum MJ, Wagner NJ. J Polym Sci, Polym Phys 1996;34:2433.
[5] Vinckier I, Moldenaers P, Mewis J. J Rheol 1996;40:613.
[6] Wening W, Meyer K. Coll Polym Sci 1980;258:1009.
[7] Stehling FC, Huff T, Speed CS, Wissler G. J Appl Polym Sci 1981;26:2693.
[8] Endo S, Min K, White JL, Kyu T. Polym Eng Sci 1986;26:45.
[9] Chen CC, Foutau E, Min K, White JL. Polym Eng Sci 1988;28:69.
[10] Ghiam F, White JL. Polym Eng Sci 1991;31:76.
[11] Chen CC, White JL. Polym Eng Sci 1993;33:923.
[12] Deeds DS, Martin JR. Rubber Plast Age 1968;69:1053.
[13] Jalbert RL, Smejkal JP. Mod Plast Encyl 1976;53:108.
[14] Freguson LE. Plast Compounding 1978;1:58.
[15] McDougle SM. Soc Plast Eng Techn Pap 1967;13:596.
[16] Grabowski TS. US Patent 3, 130, 177, assigned to Brog-Warner Corp; 1964.
[17] Hanafy GM, Madbouly SA, Ougizawa T, Inoue T. Polymer 2004;45:6879.
[18] Maxwell B. SPE J 1972;28:24.
[19] Madbouly SA, Ohmomo M, Ougizawa T, Inoue T. Polymer 1999;40:1465.
[20] Yamanaka K, Inoue T. Polymer 1989;30:662.
[21] Wu S. Polym Eng Sci 1987;27:335.
[22] Serpe G, Willis JM. J Polym Sci, Polym Phys Ed 1990;28:2259.
[23] Reijden-Stolk CV, Sara A. Polym Eng Sci 1986;26:1229.
[24] Han CD. Multiphase flow in polymer processing. New York: Academic Press; 1981.
[25] Min K, White JL. Polym Eng Sci 1984;24:1327.
[26] Taylor GI. Proc R Soc London, Ser A 1932;138:41.
[27] Taylor GI. Proc R Soc London, Ser A 1934;146:501.
[28] Grace HP. Chem Eng Commun 1982;14:225.
[29] Elmendorp JJ, Maalcke RJ. Polym Eng Sci 1985;25:1041.
[30] Elmendorp JJ. Polym Eng Sci 1986;26:418.
[31] Madbouly SA, Ougizawa T. J Macromol Sci, Phys 2002;B41:629.
[32] Madbouly SA, Chiba T, Ougizawa T, Inoue T. J Macromol Sci, Phys 1999;B38:79.
[33] Fox TG. Bull Am Phys Soc 1956;2:123.
[34] Debye P, Bueche AM. J Appl Phys 1949;20:518.
[35] Lifshits IM, Slyozov VV. J Phys Chem Solids 1961;19:35. Wagner CZ. Electrochemie 1961;65:581.
[36] Binder K, Stauffer D. Adv Phys 1976;25:343.